Effect of Counterion Competition on Micellar Growth Horizons for Cetyltrimethylammonium Micellar Surfaces: Electrostatics and Specific Binding

L. J. Magid* and Z. Han

Department of Chemistry, University of Tennessee, Knoxville, Tennessee 37996-1600

G. G. Warr and M. A. Cassidy

School of Chemistry, University of Sydney, NSW 2006, Australia

P. D. Butler and W. A. Hamilton

Solid State Division, Oak Ridge National Laboratory, Oak Ridge, Tennessee 37831-6393

Received: March 6, 1997[⊗]

Counterion-mediated micellar growth for cetyltrimethylammonium 2,6-dichlorobenzoate alone and together with cetyltrimethylammonium chloride has been investigated using small-angle scattering techniques. Variations in counterion composition at constant ionic strength cause large changes in micelle size. The selectivity coefficient for adsorption of the aromatic counterion over chloride ions at CTA^+ surfaces has been determined. The effects of the two counterions on micellar surface potentials, together with ^1H NMR chemical shift data, allow inferences to be drawn about the penetration of the aromatic counterion into the head group region of the micelles. The aromatic ion increases the surfactant-packing parameter by both increasing the average volume per surfactant monomer, a cosurfactant-like effect, and decreasing the area per head group by screening electrostatic repulsions. Counterions such as chloride, which show only surface adsorption, affect only area and are much less effective at driving micellar growth. Some comparisons are also made with literature data for CTABr.

Introduction

Using aromatic anions as counterions for cationic surfactant micelles in aqueous solution, it is possible to tune aggregate microstructure and dynamics through a range of morphologies and interactive behaviors.[1] Salicylate[2−7] (*o*-hydroxybenzoate), mono- and dichlorobenzoate ions[8] (meta- and/or para-substituted), tosylate[9,10] (*p*-methylbenzenesulfonate), and certain hydroxynaphthoate[11−13] ions are among the most effective in promoting micelle growth. Aqueous solutions of alkyltrimethylammonium salicylates ($RNMe_3Sal$) and alkylpyridinium salicylates (RPySal) in particular were among the first micellar systems[2] demonstrated to contain wormlike micelles that overlap above a characteristic concentration, c^*.

Numerical values of c^* and of micellar persistence lengths, determined by small-angle scattering and other techniques, show significant counterion specificity. Micellar dynamics in the semidilute regime, which manifest themselves in the solutions' rheological behaviors, are also exquisitely sensitive to the nature of the counterion. The magnitudes and concentration dependences (scaling law behaviors) of the observed zero-shear viscosities and longest viscoelastic relaxation times are two examples.[7−9,12,14−18] Increasing the surface charge density of pure cetyltrimethylammonium 3,5-dichlorobenzoate (CTA35ClBz) micelles by adding 30 mol % CTABr dramatically changes both the extent and kinetics of micellar alignment under Couette shear.[19]

At the other extreme are counterions such as hydroxide, fluoride, acetate, and chloride, whose $RNMe_3X$ and RPyX micelles are roughly spherical over a wide range of surfactant and salt concentrations. For CTACl in water or 0.1 M NaCl, aggregation numbers obtained using small-angle neutron scattering[20] (SANS) lie in the range of 90−120 (0.6 M CTACl was the highest concentration investigated). The salt-induced sphere-to-rod micellar transition for CTACl is assessed by light scattering[21] to occur at 1.2 M NaCl. The Debye screening length (κ^{-1}) for these solutions is ca. 0.3 nm, much smaller than the mean micellar radius of ca. 2.5 nm, so that intermicellar electrostatic repulsions are well-screened long before micellar growth starts for CTACl.

Bromide counterions occupy an intermediate position, as do some aromatic counterions. For CTABr in water,[22] micellar elongation begins at 0.12−0.15 M; Imae[23] cites the sphere-to-rod transition induced by NaBr or KBr as beginning at 0.06−0.1 M salt. The light-scattering data of Quirion and Magid[22] locate the onset of rapid micellar growth for the CTABr/KBr system at Debye lengths of 1.2−1.6 nm (0.01 M CTABr/0.07 M KBr; 0.05 M CTABr/0.035 M KBr). Delsanti and co-workers,[24] working at higher surfactant concentration and maintaining c_{salt}/c_{surf} constant, find the onset at 1.6 nm. Delsanti and co-workers have shown that the CTABr/KBr aqueous micellar system follows the theoretical predictions of Mackintosh et al.[25] concerning the effect of electrostatics on micellar growth laws.

In cationic micellar systems with mixed counterions, chloride ion at concentrations ≤1 M has generally been regarded as an indifferent electrolyte, screening electrostatic repulsions between micelles without being effective at promoting micellar elongation.[26] For 0.03 M CTABr plus 0.08 M KBr/KCl at varying mole ratios, Quirion and Magid found that the onset of micellar growth occurs at 60 mol % Br^-. This is equivalent to 0.05 M KBr: the same as found with KBr alone. Almgren and co-

* Author to whom correspondence should be addressed. E-mail address: lmagid@utk.edu.

⊗ Abstract published in *Advance ACS Abstracts,* September 1, 1997.

S1089-5647(97)00864-X CCC: $14.00

workers,[27] using viscometry and cryo-TEM, find spherical micelles only in 0.025 M CTABr in 1 M aqueous NaCl.

The degree of ionization calculated for a CTA micellar surface, using the dressed-micelle model[28] for the adsorption excess of counterions, agrees with the experimental values for Cl^-. Experimental values for Br^- are lower, and for aromatic counterions lower still (vide supra), suggesting increasing contributions from specific adsorption.

A detailed molecular-level understanding of the observed counterion specificities for aromatic counterions is very much a work in progress. Investigators are using a variety of techniques, including flotation,[29] 1D and 2D NMR,[30−33] sum-frequency vibrational spectroscopy,[34] measurements of surface potentials[35] (ψ_0), and ζ-potentials[5] to determine adsorption excesses, counterion location, and orientation for these aromatic counterions at planar and curved surfactant interfaces. Using a micelle-bound acid−base indicator in aqueous $C_{14}NMe_3Br$/NaSal, the ψ_0's associated with the plane of the head groups were determined and found to be considerably higher than the ζ-potentials, which are associated with the plane of shear. This establishes that there is more than one adsorption locus. However, it is not possible to discriminate between a model involving two discrete binding regions (intercalated among the head groups and surface adsorbed) and a continuum of adsorption/association positions. Indeed, NMR measurements in the CTA35ClBz and the cetyltrimethylammonium 2,6-dichlorobenzoate (CTA26ClBz) micellar systems[33] make it clear that small differences in counterion penetration depth and orientation apparently lead to large changes in surfactant packing and hence in micellar morphology. Thus CTA35ClBz at millimolar concentrations forms giant wormlike micelles in water.

In the present work we determine the impact on micellar structure of counterion competition between Cl^- and $26ClBz^-$ for the CTA cationic micellar surface. One extreme is the CTACl/NaCl case, which has only weak counterion binding. Addition of chloride salt is inefficient at reducing the area per molecule, a_0, at the micelle surface and hence at increasing the surfactant-packing parameter[36], v/a_0l_c, beyond $^1/_3$, the maximum value for spheres. In contrast, we expect that the micellar morphology in the CTA26ClBz system can be tuned from spheres to short rigid cylinders to large wormlike micelles at much lower concentrations of surfactant and salt. CTA26ClBz micelles in water containing no supporting electrolyte begin to grow beyond spheres at ca. 0.07 M,[8] with ^{1}H NMR chemical shifts showing clearly that counterion intercalation between the head groups (i.e., specific adsorption) is driving an increase in the v/a_0l_c.[33]

Small-angle scattering is used to assess the effects of concentrations and identity of the two counterions on micellar size, apparent micellar charge, and intermicellar repulsions. We use a variety of experimental techniques to assess overall counterion adsorption and counterion competition at CTA^+ surfaces and then make use of surface potential determinations and ^{1}H NMR chemical shifts to gain more detailed information on adsorption loci. An additional motivation of the present work was to test whether the assumption that $\leq$1 M Cl^- ions are ineffective in promoting CTA^+ micellar growth is valid regardless of the identity of the second counterion in a mixed counterion system. As we shall see, such a generalization turns out to be invalid.

Materials and Methods

Materials. The synthesis of CTA26ClBz from CTABr and sodium 2,6-dichlorobenzoate (Na26ClBz) has been described previously.[8] Elemental analysis provided the following results: CTA26ClBz, C; 65.88%; H, 9.61%; Cl, 14.84% (theoretical C, 65.79; H, 9.61; Cl, 14.94); Na26ClBz, C, 39.74%; H, 1.37%; Cl, 33.32% (theoretical, C, 39.5; H, 1.42; Cl, 33.29). A bromide ion-selective electrode was used to confirm the absence of Br^- ions. CTACl from Fluka Chemicals was used as received. Deionized water was obtained from a Millipore-Q apparatus; D_2O, 99.9 atom % D, was obtained from Aldrich Chemical Company.

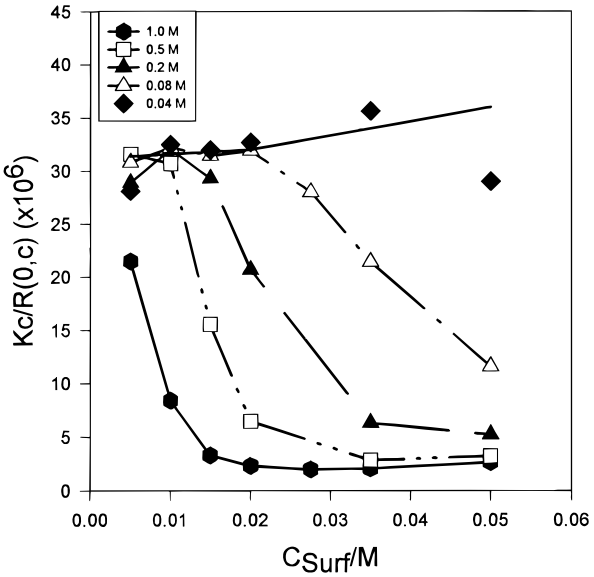

Figure 1. Static LS data for CTA26ClBz in 0.04−1 M NaCl. Lines are guides to the eye.

Na26ClBz was prepared by titration of 2,6-dichlorobenzoic acid (from TCI America) with 3N NaOH. AR grade NaCl was used as received. 4-Heptadecyl-7-hydroxycoumarin (HHC) was obtained from Molecular Probe Inc.

Static LS and SANS. Equation 1 describes the Q-dependence of the scattered intensity.

$$R(Q,c) \equiv I(Q,c) = KcM_w \cdot P(Q,c) \cdot S(Q,c) \qquad (1)$$

The collection of constants, K, is proportional in LS to the square of the refractive index increment and in SANS to the square of the contrast in scattering length density between micelle and solvent. Experimental details concerning the spectrometers used and the preliminary data processing needed in order to express the observed intensities on an absolute scale were discussed previously.[8,22] The respective Q-ranges covered in this work are 0.0085−0.031 nm^{-1} (LS) and 0.12−1.2 nm^{-1} (SANS). For the small micelles of interest here, SANS is a particularly good technique for determining aggregation numbers, $\langle n \rangle$'s, at finite c. Form factors, $P(Q,c)$'s, were computed assuming either spherical or prolate ellipsoidal micelles; the inclusion of polydispersity did not affect the results. The fitting procedures used were discussed in detail previously;[8] we simply comment here that $S(Q)$'s (intermicellar interactions) were computed using the approach of Hayter and Penfold.[37] This allows an assessment of apparent micellar charges, Z.

These micelles are small enough so that their $P(Q,c)$'s are essentially Q-invariant in the LS Q-range. However, the observed Rayleigh ratios were extrapolated to $Q = 0$. Figure 1 presents Debye plots for CTA26ClBz in aqueous NaCl. Recasting eq 1, we have $Kc/R(0,c) = (M_{w,app}(c))^{-1} = (M_w(c) \cdot S(0,c))^{-1}$, with c as the concentration of micellized surfactant. To assess the apparent Z's at c_{salt} before the onset of rapid micellar growth, we proceed according to Nicoli and co-workers:[38] assuming that micellar size (and hence M_w's)

remains roughly constant in the regime where the intermicellar electrostatic repulsions are poorly screened, $M_w(c)$ can be replaced by the (common) value $[R(0,c)/Kc]_{c=0}$ shared by the system at various low c_{salt}'s. The resulting $S(0,c)^{-1}$ values are fit using the method of Grimson and co-workers[39], eq 2:

$$S(0,c)^{-1} = 1 + 8\phi + 24\phi\cdot(U_0/kT)\cdot(1 + 2a\kappa)/(2a\kappa)^2 \quad (2)$$

$$U_0/kT = L_B Z^2/2a(1 + a\kappa)^2$$

where ϕ is the micellar volume fraction, a is the micellar radius (set at 3.2 nm, to accomodate hydration and modest deviations from sphericity), and the DLVO potential chosen is valid for $\kappa a < 3$. L_B, the Bjerrum length, is 0.71 nm at 25 °C. The second term in eq 2 is the hard-sphere contribution to the structure factor.

When c_{salt} is high enough so that $Kc/R(0,c)$ starts to decrease with increasing c, i.e., when the horizon is crossed, the micellar growth regime is considered to start. This will be referred to as the micellar growth horizon. In dilute solutions with screened electrostatic repulsions $S(0,c)^{-1}$ remains close to 1, and rapid increases in $R(0,c)$ at constant c and increasing c_{salt} can be ascribed[22,24] mainly to increasing $M_w(c)$.

For counterions such as Cl^- which are inefficient promoters of micellar growth, there is large range of c_{salt}'s above the horizon where the intermicellar electrostatic repulsions are screened but micelle growth is modest ($\kappa^{-1} \ll a$).[20,21,38] This can be tracked effectively by SANS. For very efficient promoters such as Sal^- and $35ClBz^-$, the increase in $M_w(c)$ is so dominant that the assumptions of Nicoli and co-workers are no longer valid. For intermediate cases such as Br^- and (vide infra) $26ClBz^-$, the range of c_{salt} over which micelle growth is modest narrows but does not disappear; the horizon is reached and rapid growth[24] begins when $\kappa^{-1} \approx$ a.

Methods Applied To Determine Interfacial Selectivity.

1. Ion Flotation. The experimental procedure of Morgan, et al.[29] was followed. The solution that was foamed contained initially 2.125×10^{-4} M CTACl and 1.25×10^{-4} M Na26ClBz. Samples of the solution phase were removed from the column every 15 min and analyzed by ion chromatography.

2. Proton NMR Measurements. Spectra were recorded on a Bruker AMX400 spectrometer. The proton chemical shifts (δ's) were referenced to an external standard of 10 mM DSS ($\delta = 0$) in D_2O at different NaCl concentrations, held in a capillary insert in the NMR tubes. Further details on NMR measurements in these systems are available elsewhere.[33]

3. Ion-Selective Electrode Measurements. Cl^- concentrations in micellar solutions were measured with an ORION Research model 94-17B Cl^--selective electrode and a model 900200 double-junction reference electrode. NaCl solutions were used as the standard in the calculation of Cl^- concentration. An ORION electrode-polishing strip was used to polish the electrode, which was then washed with methanol and water before each measurement.

4. Surface Potential Measurements. The micelle-bound acid−base indicator used for the ψ_0 measurements was HHC, following the procedure of Cassidy and Warr.[35] All solutions contained 0.025 M surfactant.

Results

Micellar Size and Apparent Micellar Charges from Small-Angle Scattering Data. We have repeated the static LS measurements of Imae and Ikeda,[21] confirming that CTACl micelles are still roughly spherical in 1 M NaCl. The c-dependence of $S(0,c)^{-1}$ is fit well (Figure 2a) using only the hard-sphere term in eq 2. Fitting a series of $S(0,c)^{-1}$ vs c curves at various lower c_{NaCl}'s, Nicoli and co-workers[38] found α values ($Z/\langle n\rangle$) of 0.24−0.27 for CTACl/NaCl. Assuming an aggregation number of 100, this suggests an apparent micellar charge of 24−27.

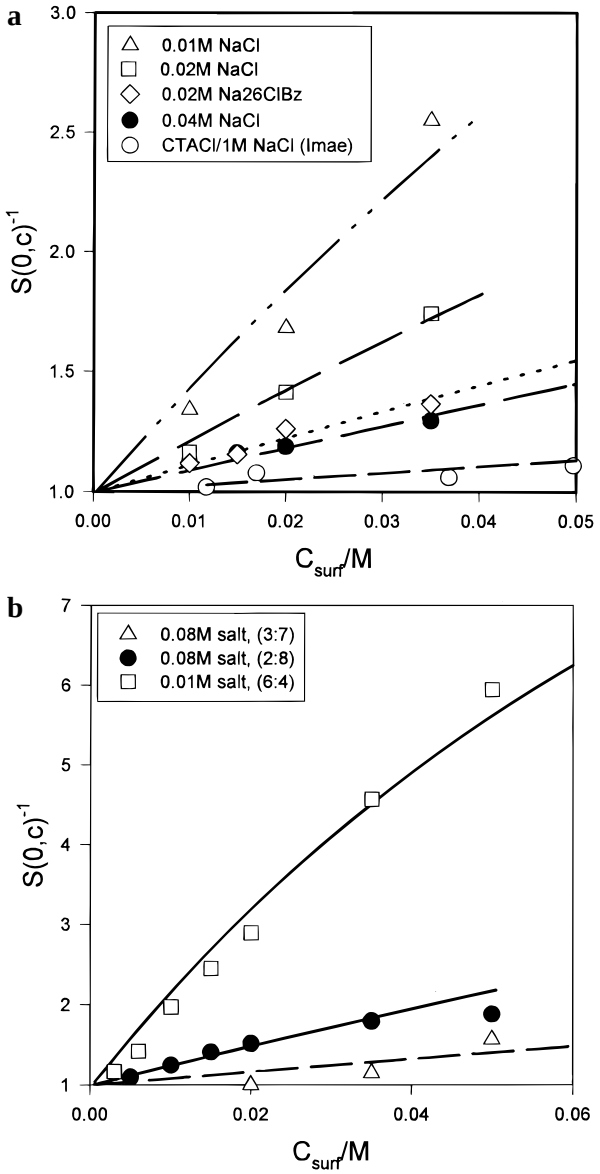

Figure 2. Fit of LS-derived micellar structure factors $S(0,c)^{-1}$ below the micellar growth horizon. (a) CTA26ClBz in aqueous NaCl and Na26ClBz. Also shown for comparison are results for CTACl in 1 M NaCl.[21] (b) Mixed micelles of CTA26ClBz/CTACl in Na26ClBz/NaCl salt. Total molar ratios of $26ClBz^-$ to Cl^- in the solutions are given in parentheses.

From static LS results, the micellar growth horizons for CTA26ClBz micelles in aqueous NaCl (Figure 1) and in aqueous Na26ClBz are much lower: ca. 0.08 M and 0.025 M salt, respectively. $S(0,c)^{-1}$'s for 0.04 M NaCl and 0.02 M Na26ClBz are presented in Figure 2a, together with the results of fits to eq 2 in Table 1. Apparent Z's of 13.5 ± 0.6 and 10.3 ± 0.4 are obtained for these two CTA26ClBz systems.

The three additional systems presented in Figure 2b are prepared using CTACl and CTA26ClBz and their Na salts to contain constant molar ratios of $Cl^-/26ClBz^-$; total [NaX] is 0.08 M. At 70 and 80 mol % CTACl, 0.08 M salt is still in the repulsive regime, with a significantly larger Z (34−40 vs 19) for the system with the higher mole percent of Cl^-. The salt concentration in these two systems is high enough to dominate

TABLE 1: Apparent Micellar Charges below the Micellar Growth Horizon and Values of c_{salt} at the Horizons As Assessed by Static LS

surfactant	salt	c_{salt}/M	apparent Z	c_{salt} at horizon/M
CTACl	NaCl			1.2[a]
CTA26ClBz	NaCl	0.01, 0.02[b]	15.6 ± 0.4	
	NaCl	0.04	13.5 ± 0.6	ca. 0.08
	Na26ClBz	0.02	10.3 ± 0.4	ca. 0.025
CTA26ClBz/CTACl (3:7)	Na26ClBz/NaCl	0.08	19.3 ± 5.9	ca. 0.1
(2:8)		0.02,0.05,0.08[b]	33.9 ± 0.4	
(2:8)		0.08	40.2 ± 0.8	
(6:4)		0.01	26.5 ± 0.6	ca. 0.025

[a] Reference 21. [b] These curves fitted together.

TABLE 2: Micellar Aggregation Numbers and Apparent Micellar Charges Derived from SANS Measurements

c/M	c_{salt}/M	$\langle n \rangle$	Z	a_{tot}/nm	κ^{-1}, nm	χ
0.02		104 ± 1	16.6 ± 0.3	2.79	7.3	2.26
	0.01 M NaCl	132 ± 1	19.6 ± 0.5	3.02	2.8	1.56
	0.02 M NaCl	142 ± 2	21.0 ± 0.9	3.10	2.1	2.13
	0.05 M NaCl	180 ± 3		3.45	1.4	1.45
0.05		114 ± 1	19.9 ± 0.2	2.87	4.6	2.13
	0.01 M NaCl	141 ± 1	18.7 ± 0.3	3.10	2.6	1.63
	0.02 M NaCl	212 ± 3	14.1 ± 0.4	3.58	2.1	1.57
0.01		105 ± 2	13.2 ± 0.7	2.81	9.0	1.55
	0.02 M Na26ClBz	180 ± 6	11.6 ± 2.1	3.39	2.1	1.27
	0.04 M Na26ClBz[a]	290 ± 7			1.5	2.05
0.02	0.01 M Na26ClBz	140 ± 2	17.8 ± 0.7	3.10	2.9	1.44
	0.02 M Na26ClBz	214 ± 6	7.9 ± 1.1	3.60	2.1	1.84
0.035		114 ± 1	19.1 ± 0.4	2.88	5.2	1.53
	0.01 M Na26ClBz	146 ± 2	18.7 ± 0.5	3.14	2.7	1.57
	0.02 M Na26ClBz	289 ± 8		4.0	2.1	2.96

[a] Fit assuming cylindrical micelles.

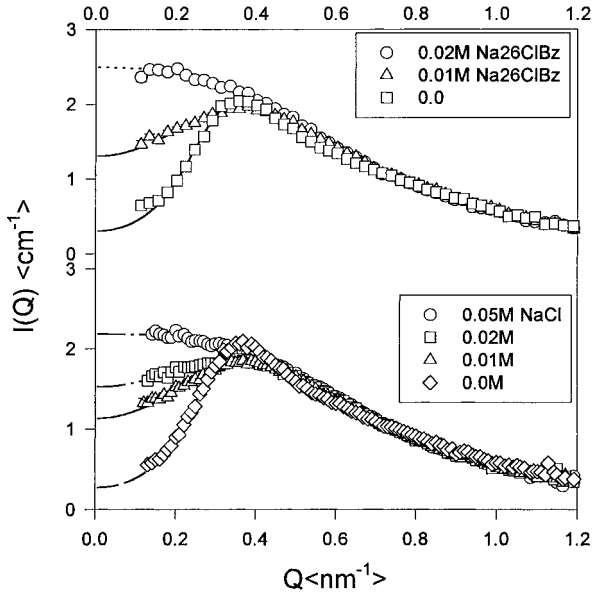

Figure 3. Results of fitting SANS data for 0.02 M CTA26ClBz in aqueous Na26ClBz and in aqueous NaCl.

the solutions' Debye lengths (κ^{-1}). By the time the CTACl content decreases to 40 mol %, the horizon occurs at ca. 0.025 M salt, essentially the value for pure CTA26ClBz/Na26ClBz. Figure 2b presents the data at 0.01 M salt for this third system; a fitted Z of 26.5 ± 0.6 is obtained.

A comparison of $\langle n \rangle$'s and Z's for CTA26ClBz in aqueous NaCl and aqueous Na26ClBz assessed by static SANS measurements is presented in Table 2. Figure 3 illustrates typical fits of the experimental data, focusing on 0.02 M CTA26ClBz. The common ion salt at 0.02 M results in a micellar solution lacking a peak in its scattering curve, but a peak in $I(Q)$ (and hence in $S(Q)$) persists at 0.02 M NaCl. As expected, micellar growth is also more rapid in the presence of Na26ClBz than NaCl. From

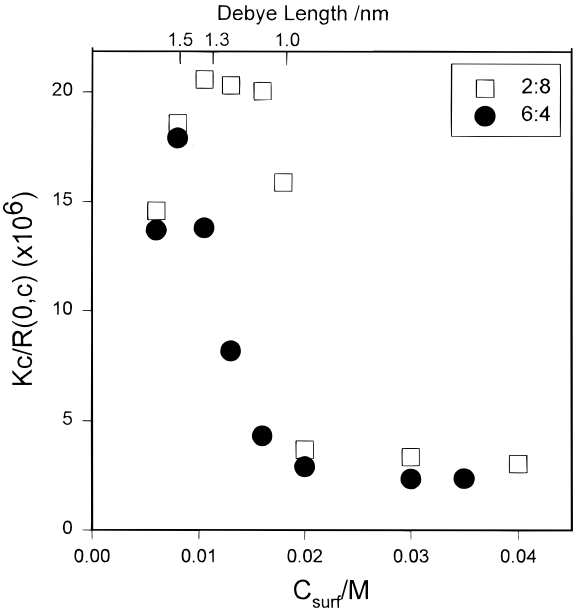

Figure 4. Static LS for mixed micelles of different ratios of CTA26ClBz/CTACl in aqueous Na26ClBz/NaCl solutions. Total molar ratios of $26ClBz^-$ to Cl^- in the solutions are given in parentheses. Systems are compared at matched Debye screening lengths (κ^{-1}/nm).

Table 2, the SANS-derived Z's at 0.01 and 0.02 M CTA26ClBz in 0.02 M Na26ClBz are 11.6 and 7.9, respectively, in reasonable agreement with the values determined by LS. The SANS results of course demonstrate that $\langle n \rangle$ increases slightly with increasing c, even in the repulsive regime.

The calculated degree of ionization ($\alpha = 0.25-0.26$) of a CTA micellar surface[28] ($A_{hg} = 0.72$ nm^2) agrees with the SANS-determined[20] α for CTACl in the absence of salt, 0.24−0.28. This confirms the lack of specific adsorption of Cl^-. The SANS-determined α's for CTA26ClBz micelles in the absence of salt are 0.13−0.17, significantly lower. Conductimetry measurements[40] give 0.16 for CTA26ClBz in water. Bromide[22] ions show a similar, although smaller, deviation, again with $\alpha_{expt} < \alpha_{calc}$. In 0.05−0.6 M CTACl in the presence of 0.1 M NaCl, the SANS-determined α remains above 0.2,[20] again in marked contrast to the situation for CTA26ClBz.

A Delsanti Experiment: Micelle Size at Constant Debye Screening Lengths. The static LS results presented in Figure 2b suggested that we should explore the specific adsorption of 2,6-dichlorobenzoate ions further by investigating the effect of changing the 26ClBz/Cl molar ratio on micelle size at constant κ^{-1}. Figure 4 shows the static LS results for the mixed surfactant, mixed salt system with 80 and 40 mol % chloride and c_{salt}/c_{surf} constant at five. As eq 3

$$\kappa^2 = 4\pi L_B c \cdot (\alpha + 2c_{salt}/c) \qquad (3)$$

makes clear, this surfactant-to-salt ratio determines κ^{-1}, since

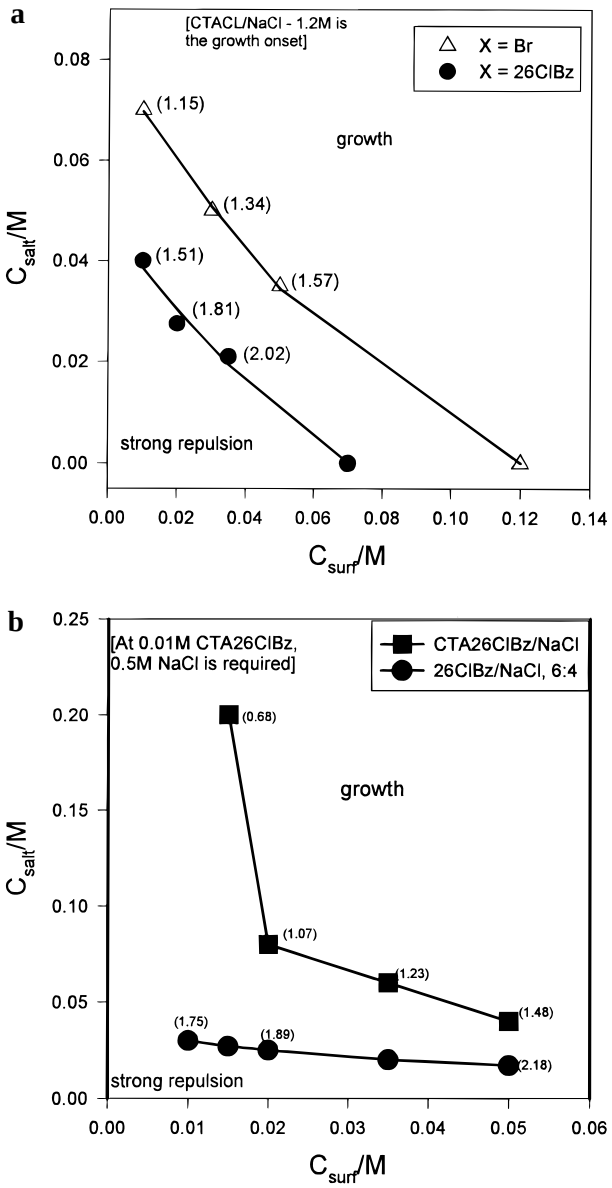

Figure 5. Micellar growth and interaction diagrams. Data points separate spherical micelles (below) from rod-growth region (above). (a) For CTABr/KBr and CTA26ClBz/Na26ClBz; (b) for CTA26ClBz with NaCl and for the mixed system (6:4) CTA26ClBz/CTACl with mixed salt. Figures in parentheses are the Debye lengths (nm).

a is certainly less than 0.2. At $\kappa^{-1} > 1.5$ nm, electrostatic repulsions dominate and $Kc/R(0)$ increases with increasing surfactant concentration. Examining the region where 1.5 nm $> \kappa^{-1} > 0.96$ nm, we see a marked difference in the onset of rapid micellar growth: at $\kappa^{-1} = 1.5$ nm in the 6:4 $26ClBz^-/Cl^-$ system, but not until $\kappa^{-1} = 1.0-1.07$ nm in the 2:8 system.

Micellar Interaction and Growth Diagrams. Constructed from the static LS data, these diagrams provide a convenient visual representation of the effects of various counterions in the CTA^+ micellar system. An increase in surfactant concentration results in a decrease in the c_{salt} at which the rapid increase in $R(0,c)$ (dominated by M_w) begins. Figure 5a compares Br^- and $26ClBz^-$; recalling that CTACl micelles are still spherical at $\kappa^{-1} = 0.3$ nm, we have the series $Cl^- \gg Br^- > 26ClBz^-$ in terms of the concentration of salt or decrease in Debye screening length needed for the onset of growth. For the mixed system of CTA26ClBz/NaCl (Figure 5b), κ^{-1} evolves as c_{surf} increases from close to the value in the pure Cl^- system (0.43 vs 0.3 nm), to values more characteristic of the pure $26ClBz^-$ system. For CTA26ClBz/NaCl and CTA26ClBz/Na26ClBz, the SANS

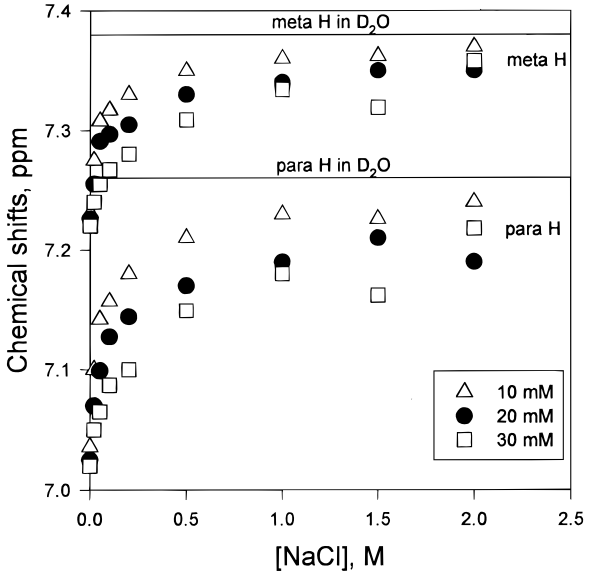

Figure 6. Proton NMR data for CTA26ClBz in aqueous NaCl: aromatic protons of the $26ClBz^-$ counterions.

results in Table 2 are consistent as well with the interactions/growth boundaries. For the mixed system at 6:4 CTA26ClBz/CTACl, the κ^{-1} values are essentially the same as for the pure $26ClBz^-$ system. For 2:8 CTA26ClBz/CTACl, we do not have static LS data at salt concentrations below the horizon in Figure 2b. However, given that the horizon occurs in the vicinity of 0.1 M salt (Table 1) and given the results in Figure 4, we can estimate that κ^{-1} on the order of 1.0 nm is needed for growth in this case.

Determination of the $26ClBz^-/Cl^-$ Selectivity Coefficient at the CTA^+ Solution/Air Interface. The flotation technique of Morgan et al.[29] measures a selectivity coefficient for two counterions X^- and Y^-, $K = ([Y^-]/[X^-])_{int} \cdot ([X^-]/[Y^-])_{bulk}$, that is numerically equal to the thermodynamic ion exchange equilibrium constant. The technique has been demonstrated to produce K's that are independent of bulk solution composition and surface charge density. The evolution of $[26ClBz^-]$ and $[Cl^-]$ remaining in the solution phase as foaming proceeds is fit well by:

$$\ln[26ClBz^-]_{bulk} = K \ln[Cl^-]_{bulk} + C \qquad (4)$$

The value obtained for K is 16.8 ± 1.0.

Estimation of K for CTA^+ Micellar Surfaces. For micellar surfaces, values of selectivity coefficients are technique-dependent, just as determinations of the extent of counterion adsorption are, because different aspects of the micelle−counterion interactions are probed.[41] Spectroscopic techniques such as NMR generally detect only counterions closest to the micellar surface, not those in the diffuse double layer. In contrast, ion-selective electrodes detect only free counterions in the bulk phase.

Displacement of $26ClBz^-$ ions (Y^-) from the CTA^+ micellar surface upon addition of Cl^- ions (X^-) was monitored by proton NMR for solutions of 0.01, 0.02, and 0.03 M CTA26ClBz in aqueous NaCl (0−2 M). Association of the $26ClBz^-$ ion with the micelles shields the aromatic protons (Figure 6), as previously observed for CTA26ClBz micelles in water.[33] Even at [NaCl] ≥ 1 M, some $26ClBz^-$ ions remain on the surface. To estimate K, $26ClBz^-$ and Cl^- are assumed to undergo a 1:1 exchange, with α remaining constant at 0.15, the value for CTA26ClBz in the absence of NaCl. Further, since NMR is likely to detect only those $26ClBz^-$ ions penetrating the head

TABLE 3: Assessment of Counterion Competition for the CTA^+ Micellar Surface Using Proton NMR: CTA26ClBz/NaCl

c/M[a]	c_{NaCl}/M	δ_{obs}/ppm	$[26ClBz^-]_b/[26ClBz^-]_f$[b,c]	$[Cl^-]_f/[Cl^-]_b$	K
			Para Proton		
0.010	0.020	7.100	1.54	7.23	11.2
	0.050	7.142	0.812	11.4	9.3
	0.10	7.157	0.642	20.8	13.3
	0.20	7.180	0.437	35.6	15.5
	0.50	7.210	0.176	70.4	12.4
	1.0	7.230	0.129	135.	17.4
0.020	0.020	7.070	2.195	5.13	11.3
	0.050	7.099	1.392	8.33	11.6
	0.10	7.127	0.927	12.6	11.7
	0.20	7.144	0.724	22.3	16.1
	0.50	7.170	0.483	46.6	22.5
	1.0	7.190	0.339	82.8	28.1
0.030	0.020	7.050	2.920	5.35	15.6
	0.050	7.065	2.247	9.55	21.5
	0.10	7.087	1.591	13.1	20.9
	0.20	7.100	1.315	22.6	29.7
	0.50	7.149	0.650	35.5	23.1
	1.0	7.180	0.397	57.9	23.0
			Meta Protons		
0.010	0.020	7.275	1.506	7.03	10.6
	0.050	7.308	0.701	10.4	7.3
	0.10	7.317	0.565	19.4	11.0
	0.20	7.330	0.403	34.5	13.9
	0.50	7.350	0.209	72.9	15.2
	1.0	7.360	0.131	135.	17.7
0.020	0.020	7.255	2.236	5.29	11.8
	0.050	7.291	0.968	5.98	5.8
	0.10	7.297	0.848	11.8	10.0
	0.20	7.305	0.709	22.0	15.6
	0.50	7.330	0.383	42.6	16.3
	1.0	7.340	0.285	78.4	22.3
0.030	0.020	7.240	2.922	5.35	15.6
	0.050	7.255	1.985	8.01	15.9
	0.10	7.267	1.513	12.4	18.8
	0.20	7.280	1.137	20.0	22.7
	0.50	7.309	0.608	34.3	20.9
	1.0	7.334	0.326	54.2	17.7

[a] $[CTA^+]_{mic}$ is set equal to the total surfactant concentration. The cmc for CTA26ClBz in the absence of salt is 5.6×10^{-4} M.[8,40] [b] Values of δ_b for the para H are 6.996 ppm (0.01 M surfactant), 6.984 (0.02 M), 6.978 (0.03 M); for the meta H's: 7.205; 7.199; 7.192. [c] Values of δ_f are 7.260 ppm (para H); 7.380 ppm (meta H).

group region, a two-site model is used: counterions are either free in bulk solution or in a single, average micellar environment. Assuming rapid equilibration of counterions between the two environments, $[26ClBz^-]_b/[26ClBz^-]_f \equiv P_b/P_f$ can be determined according to:

$$\delta_{obs} = P_f\delta_f + P_b\delta_b \quad (5)$$

Values for δ_f were measured directly; values for δ_b were calculated from eq 5 using values of δ_{obs} measured at each surfactant concentration in the absence of NaCl and setting P_f equal to α. Free and bound Cl^- are derived as follows:

$$[Cl^-]_b = (1 - \alpha)\cdot[CTA^+]_{mic} - [26ClBz^-]_b \quad (6)$$

$$[Cl^-]_f = [Cl^-]_{tot} - [Cl^-]_b$$

Table 3 presents the values of $K_{26ClBz/Cl}$ obtained using chemical shift data for both the meta protons and the para proton. The average of all K's reported is 16.2 ± 5.5. Below the micellar growth onset, the average is 12.5 ± 3.4, while values up to 30 are observed in the micellar growth regime. The results are suggestive of enhanced selectivity for $26ClBz^-$ ions as the micelles grow beyond minimum spheres.

TABLE 4: Assessment of Counterion Competition for the CTA^+ Micellar Surface: 0.01 M CTACl/Na26ClBz

c_{salt}/M	$[Cl^-]_f/[Cl^-]_b$[a]	$[CTA^+]_{mic}$/M[b]	α[c]	$[26ClBz^-]_b/[26ClBz^-]_f$	K
0	0.587	0.0090	0.30	–	–
0.0005	0.639	0.0091	0.292	2.09	1.3
0.0010	0.686	0.0092	0.285	1.78	1.2
0.0020	0.800	0.0094	0.27	1.76	1.4
0.0040	0.975	0.0097	0.24	1.41	1.4
0.0050	1.11	0.0099	0.225	1.44	1.6
0.0070	1.67	0.00995	0.195	1.55	2.6
0.010	2.45	0.010	0.15	1.26	3.1
0.015	5.25	0.010	0.11	0.943	5.0
0.020	11.5	0.010	0.075	0.732	8.4

[a] $[Cl^-]_f$ directly from measurement with Cl^--selective electrode; $[Cl^-]_b = 0.01 - [Cl^-]_f$. [b] cmc's were determined at 0 M Na26ClBz, 0.0010 M; at 0.005 M, 7.0×10^{-5} M; at 0.010 M, 2.6×10^{-5} M. Values at the remaining salt concentrations were interpolated. [c] Degrees of ionization are interpolated from the experimental values of $\alpha = 0.3$ in CTACl (ISE) and $\alpha = 0.15$ for CTA26ClBz in 0.01 M NaCl (SANS, see Table 2).

TABLE 5: Micellar Surface Potentials Determined Using HHC

surfactant[a]	salt	c_{salt}/M	ψ_0/mV	ζ potential/mV
TTABr[b]			165.5	67
	NaSal	0.01		42
	NaSal	0.025	87.8	
	NaSal	0.05		5.4
	NaSal	0.10	37.8	−3.1
CTACl			150	92
	NaCl	1.0	80	
CTABr			140[c]	
			156[d]	
	KBr[d]	0.01	130	
	KBr	0.05	105	
	KBr	0.10	92	
CTA26ClBz			125	76
	Na26ClBz	0.01	94	65
	Na26ClBz	0.05	65	55
	Na26ClBz	0.10	51	30
	NaCl	0.05	111	55
	NaCl	0.10	104	48
	NaCl	1.0	71	

[a] 0.025 M surfactant except as noted. [b] Reference 35. [c] Reference 42; 0.05 M CTAB. [d] Reference 43; 0.005 M CTABr, using $E_T(30)$ as the indicator.

We also attempted to use a Cl^--selective electrode to follow the displacement of Cl^- ions from the micelles in 0.01 M CTACl as Na26ClBz was added. In this case, $[Cl^-]_f/[Cl^-]_b$ is determined directly and $[26ClBz^-]_b/[26ClBz^-]_f$ is derived; Table 4 tabulates the results. Estimating the amount of $26ClBz^-$ associated with the micelles required assumptions about α; clearly it will decrease as $26ClBz^-$ is added, so that more than a true 1:1 ion exchange is occurring. We used the experimental values of 0.30 at zero added Na26ClBz and 0.15 at 0.01 M added Na26ClBz (from SANS), and we assumed that α is directly proportional to [Na26ClBz]. Not surprisingly, we find a salt-dependent K. It is 1.3 ± 0.1 up to 0.004 M Na26ClBz, increasing rapidly at higher salt; the values are generally considerably lower than those obtained for 0.01 M surfactant using NMR. Measurements were not possible at higher [CTACl]'s because of fouling of the electrode surface by the surfactant. The electrode's response also showed increasing deviations from Nernstian behavior as [Na26ClBz] increased.

Micellar Surface Potentials and ζ-Potentials. Table 5 presents the results obtained in this investigation on CTACl and

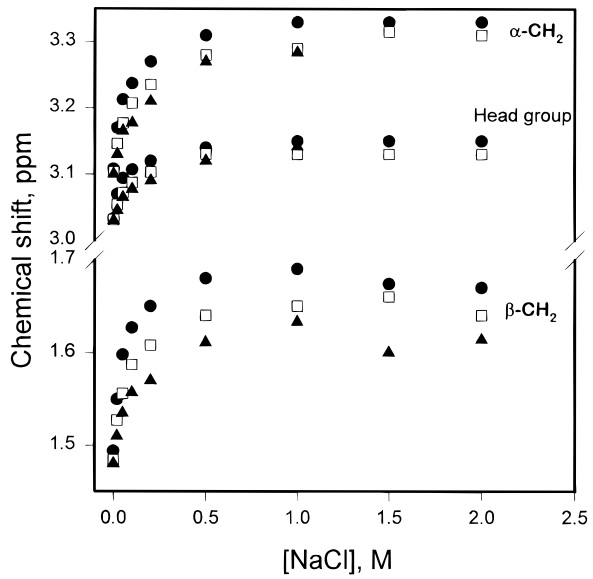

Figure 7. Proton NMR data for the surfactant ions in CTA26ClBz/NaCl: α-H's, head group H's and *β*-H's.

CTA26ClBz, as well as, for purposes of comparison, data from the literature for TTABr/NaSal[35] and CTABr/KBr.[42,43] For 25 mM surfactant solutions without added salt, the measured ψ_0's decrease for the series CTACl, CTABr, CTA26ClBz. This is in the same order as their α values assessed by various experimental methods (scattering, conductimetry, ion-selective electrodes, etc.). The higher the ψ_0 measured at 0.025 M, the higher the c or c_{salt} required for the onset of micellar growth.

The observed drop in ψ_0 when 0.1 M NaX is added for three systems is largest for TTABr/NaSal at 128 mV and smallest for CTA26ClBz/NaCl at 46 mV, with the $26ClBz^-$ anion occupying the intermediate position, a drop of 74 mV for CTA26ClBz/Na26ClBz. In each case, c_{salt} dominates the Debye screening length; κ^{-1} is 0.96 nm at 0.1 M NaX. As was the case for the salt-free systems, the observed decreases in ψ_0 parallel the counterions' ability to promote micellar growth.

Using the data in the growth and interaction diagram of Figure 5a, at 0.025 M CTA26ClBz ca. 0.03 M Na26ClBz or 0.07 M NaCl is required for the onset of significant micellar growth. Table 3 allows us to estimate the drops in ψ_0 associated with these growth onsets as 45 and 42 mV, respectively. A similar decrease[43] in ψ_0 (50−55 mV) has been observed at 0.005 M CTABr in aqueous KBr, a system whose growth onset is at ca. 0.06 M KBr. In 1.0 M NaCl, where κ^{-1} is 0.3 nm and the micellar double layer is thin, the ψ_0's are approximately the same for 0.025 M CTACl and 0.025 M CTA26ClBz, solutions that contain, respectively, spherical micelles and semiflexible threadlike micelles.[44]

At 0.025 M in salt-free solution, CTACl and CTA26ClBz have measured ζ-potentials of 92 and 76 mV, respectively, values that parallel assessments by other techniques of their relative micellar charges. The observed decrease in ζ-potential as Na26ClBz or NaCl is added is much less sensitive to the identity of the counterion than is the case for the ψ_0's. There is no evidence for charge reversal, as observed for the TTABr/NaSal couple.

For the CTA26ClBz/Na26ClBz system, the measured ζ-potentials are always lower than the ψ_0's, which indicates that there is a population of $26ClBz^-$ ions beyond the head group region in surface-adsorbed sites.

Counterion Localization and Orientation. NMR chemical shifts for the protons of the N-methyl groups and C-1 (α) and C-2 (*β*) of the alkyl chains are presented (Figure 7) for 0.01, 0.02, and 0.03 M CTA26ClBz in NaCl solutions. Significant shielding of all three groups of protons is observed because of the effect of the counterions' aromatic ring current. As $26ClBz^-$ ions are displaced by Cl^- ions, the δ_{obs}'s reach plateaus at ca. 1 M NaCl. The three groups of protons are still in shielded environments relative to those in CTACl micelles, either spheres or rods, suggesting, as do the δ's of the counterions themselves, that some fraction of the $26ClBz^-$ ions are still associated with the micellar surfaces, penetrating the head group region, at high [NaCl].

Discussion

For CTABr micellar solutions, promotion of growth by adding Cl^- is similar to what is observed for CTACl: micelles of both CTABr and CTACl (at 0.01−0.05 M surfactant) in aqueous NaCl remain roughly spherical[23,27] up to 1 M NaCl. A value of $K_{Br/Cl}$ in the range of 2−3 suggests substantial exchange of Cl^- for Br^- as the reason. The ineffectiveness of Cl^- ions in promoting growth is also seen at constant ionic strength: at 0.03 M CTABr, where ca. 0.05 M Br^- is needed for the onset of micellar growth (Figure 5 and ref 22), the micelles remain small in a mixed 0.08 M salt solution (Br^-/Cl^-) until the Br^- concentration reaches 0.05 M. This is consistent with Cl^- ions being predominantly surface-adsorbed, and with the full micellar population of Br^- ions, of which only a few are involved in penetration of the head group region, being displaceable from the micellar surfaces.

Both the rate of ψ_0 lowering for CTAX micelles as NaX or KX is added and the decline in α's determined by various techniques for salt-free solutions—Cl^-, 0.25−0.30; Br^-, 0.20−0.25; $26ClBz^-$, 0.13−0.17—make it clear that chemical contributions (specific adsorption) as well as electrostatic contributions are important in understanding micellar interactions and growth in these systems. Of the three counterions, $26ClBz^-$ is the most effective at penetrating the head group region. Added Cl^- acts only to increase the surfactant-packing parameter by decreasing a_0; Br^- acts primarily on a_0 as well. In contrast, added $26ClBz^-$ both decreases a_0 and increases v.

CTA26ClBz/Cl micellar solutions therefore behave differently from CTABr/Cl micellar solutions. Depending on the CTA26ClBz concentration, added Cl^- ions are quite effective at promoting micellar growth (see Figure 5), although less effective than $26ClBz^-$ ions themselves. The micellar growth horizon for 0.01 M CTA26ClBz occurs at 0.5 M NaCl; by 0.02−0.03 M CTA26ClBz, only 0.06−0.08 M NaCl is needed, in complete contrast to the case of CTABr. Given the selectivity coefficients of 16 for $26ClBz^-/Cl^-$ and 3 for Br^-/Cl^-, one sees that 0.01 M CTAX micelles in 0.5 M NaCl have micellar surfaces with 19% adsorbed $26ClBz^-$ vs 4% adsorbed Br^-; for 0.02 M CTAX in 0.08 M NaCl, the corresponding numbers are 66% and 37%.

The greater ability of the $26ClBz^-$ ions to penetrate the head group region leads to changes in micelle morphology at lower loadings of the micelle surface than needed in the case of more weakly penetrating counterions such as Br^- or nonpenetrating counterions like Cl^-. The ability of the $26ClBz^-$ ions to increase v/a_0l_c and hence promote the transition to rigid and then flexible cylindrical micelles is especially clear at high ionic strength. In 1 M NaCl, where the micelles' diffuse double layers are thin and the comparable ψ_0's for 0.025 M CTACl and 0.025 M CTA26ClBz suggest comparable surface charge densities, only the system having intercalating counterions is well into the micellar growth regime.

In the mixed surfactant, mixed salt systems (constant overall molar ratio of 26ClBz/Cl) reported in Table 1 and in Figures 4

and 5, behavior distinct from that of the Br/Cl couple persists. At 0.02 M surfactant, the onset of micellar growth (Figure 5) occurs at a κ^{-1} of 1.8−1.9 nm, both for 26ClBz$^-$ as the sole counterion present and for the case of 6:4 26ClBz$^-$/Cl$^-$. This is completely consistent with $K_{26ClBz/Cl} = 16$, which suggests that in the 6:4 series, 95% of the adsorbed counterions are 26ClBz$^-$. For the 2:8 series, where only 20 mol % of the total counterions present are 26ClBz$^-$, they represent 68% of the adsorbed counterions. Comparison of the two series (Figure 4) shows that for 0.08−0.02 M surfactant there is a range of κ^{-1}'s (set by the ratio c_{salt}/c) where increasing mole percent CTA26ClBz at constant CTA$^+$ concentration results in increasing micelle size. Equivalently, a lower 26ClBz$^-$ content in these mixed systems requires more extensive screening (a lower value of κ^{-1}) at the onset of micellar growth. At 20 mol % 26ClBz$^-$, growth starts at 0.016−0.018 M surfactant and 0.08−0.09 M salt, where κ^{-1} is 1.1 nm; at 60 mol % 26ClBz$^-$, the corresponding concentrations are 0.008 and 0.04 M and κ^{-1} is 1.5 nm.

As the loading of the micellar surface with 26ClBz$^-$ ions increases, changes in micellar morphology can occur at lower and lower total salt concentrations. For aromatic counterions such as 35ClBz$^-$ or Sal$^-$ that form giant wormlike micelles with CTA$^+$ even in salt-free solutions, the surface loadings of the aromatic counterions needed in mixed systems with CTACl/NaCl are likely to be lower still.

Chloride ions themselves adsorb primarily at the micellar surface, rather than penetrating the head group plane. To consider further how Cl$^-$ promotes micelle growth at low loadings of a second counterion such as 26ClBz$^-$, but not Br$^-$, we need to look more closely at the details of adsorption sites for aromatic counterions. What can we say with confidence about the distribution of the 26ClBz$^-$ ions among various adsorption loci? One locus (locus #1) definitely involves intercalation of the head groups, as a consideration of ψ_0's makes clear. We can also say that locus 1 is not saturated with 26ClBz$^-$ ions, since the ψ_0's drop significantly as Na26ClBz is added. A second locus (locus 2) is surface adsorption. As noted in the Results section, the single-counterion system CTA26ClBz/Na26ClBz has counterions occupying both loci. The measured ζ-potentials for CTA26ClBz/NaX solutions suggest that total counterion adsorption is weakly dependent on whether X is 26ClBz$^-$ or Cl$^-$. Thus some adsorbed 26ClBz$^-$ counterions must be in locus 2 as well. In fact, it is likely that there is a continuum of adsorption sites, with a considerable distribution of the aromatic counterions about an average depth of penetration.

The ^{1}H δ's are consistent with the assertion that 26ClBz$^-$ ions occupy both penetrating and surface adsorption loci for micelles in salt-free solutions, given the size of the shielding effects ($\delta_f - \delta_b$) experienced by the aromatic ring protons. The strongest intercalators, such as Sal$^-$ and 35ClBz$^-$ ions, are those that produce the largest drops[45] in ψ_0's. Para protons of the strongest intercalators show the largest shielding effects, 0.42 ppm for salicylate[32b] with TTA$^+$ and 0.40 ppm for 3,5-dichlorobenzoate[46] with CTA$^+$. In contrast, for 0.01−0.03 M CTA26ClBz the value is 0.27 ppm and for TTA *o*-nitrobenzoate,[32b] which has binding characteristics similar to CTA26ClBz, the value is 0.22. The difference in magnitudes of shielding, ca. 0.27 ppm for 26ClBz$^-$ versus 0.4 ppm for 35ClBz$^-$, can be taken to suggest that the partitioning between locus 1 and locus 2 favors locus 1 less strongly in the case of 26ClBz$^-$.

Unfortunately, the ortho protons of even the strongest intercalators show little change in δ's upon transfer from water to the micellar environment, suggesting that they remain in a hydrated milieu. This fact suggests that occupation of surface adsorption sites by aromatic ring protons of surface-adsorbed aromatic counterions is unlikely to be detectable directly by ^{1}H NMR: $\delta_{b,2}$ is likely to be close (within 0.1ppm) to δ_f. It is also not possible to detect increased partitioning of 26ClBz$^-$ ions into locus 1 as Cl$^-$ ions are added, nor is it possible therefore to infer that in the mixed 26ClBz$^-$/Cl$^-$ systems, 26ClBz$^-$ ions are only in locus 1 while Cl$^-$ ions are only in locus 2.

The differential shielding of para protons discussed above may also indicate that the average depth of penetration into the micellar surface is greater and/or that the extent of micellar surface roughness is different for the counterions producing the largest drops in ψ_0. Our previous NMR work on CTA26ClBz/CTABr and CTA35ClBz/CTABr mixed micellar systems suggests that these effects are very difficult to disentangle.

Conclusions

The aromatic counterion 2,6-dichlorobenzoate penetrates the head group region of CTA$^+$ micelles, lowering the surface potentials of the micellar surfaces and causing an increase in the surfactant-packing parameter by decreasing a_0 and also increasing v. As a result, this aromatic counterion, as well as other more strongly binding examples such as salicylate and 3,5-dichlorobenzoate, produces micellar growth at much lower ionic strengths than surface-adsorbing counterions such as Cl$^-$. The onset of micellar growth for weakly penetrating counterions such as Br$^-$ occurs when the Debye screening length and the micellar radius are comparable. Given their higher selectivity coefficient for the micellar surface, 2,6-dichlorobenzoate ions move micellar growth horizons to still lower values of κ^{-1}. Because of the differences in K's, compared to CTABr solutions containing a given concentration of Cl$^-$, CTA26ClBz solutions have micellar surfaces that retain a higher content of the aromatic counterion. The nature of its adsorption by penetration among the surfactant head groups holds the key to micellar growth: when the ionic strength is high (e.g., in 1 M NaCl), similar surface potentials can produce very different micellar morphologies, with CTACl micelles remaining spherical while CTA26ClBz micelles show extensive growth.

Acknowledgment. Work at the University of Tennessee and at Oak Ridge National Laboratory was supported by the U.S. Department of Energy under Contract No. DE-AC05-96OR22464 with Lockheed Martin Energy Research Corporation. Parts of this work at the University of Sydney were funded by the Australian Research Council Institutional Grants Scheme. M.A.C. acknowledges receipt of an ARC postgraduate scholarship. The SANS data were acquired at the W.C. Koehler 30m SANS facility at Oak Ridge National Laboratory, supported by the U.S. Department of Energy, Division of Materials Science under Contract No. DE-AC05-840R21400.

References and Notes

(1) (a) Cates, M. E.; Candau, S. J. *J. Phys.: Condens. Matter* **1990,** *2*, 6869 and references therein. (b) Rehage, H.; Hoffmann, H. *Mol. Phys.* **1991**, *74*, 933 and references therein. (c) Porte, G. in *Micelles, Membranes, Microemulsions and Monolayers*; Gelbart, W. M.; Ben-Shaul, A.; Roux, D., Eds.; Springer-Verlag: New York, 1994; Chapter 2.

(2) (a) Kalus, J.; Hoffmann, H.; Reizlein, K.; Ulbricht, W.; Ibel, K. *Ber. Bunsen-Ges. Phys. Chem.* **1982**, *86*, 37. (b) Rehage, H.; Hoffmann, H. *Faraday Discuss. Chem. Soc.* **1983**, *76*, 363. (c) Hoffmann, H.; Rehage, H.; Reizlein, K. Thurn, H. *Proceedings of the ACS Symposium on Macro- and Microemulsions;* American Chemical Society: Washington, DC, 1985; p 41.

(3) (a) Wan, L. S. C. *J. Pharm. Sci.* **1966**, *55*, 1395. (b) Gravsholt, S. *J. Colloid Interface Sci.* **1976**, *57*, 575. (c)Ulmius, J.; Wennerström, H.; Johansson, L. B.-Å; Lindblom, G.; Gravsholt, S. *J. Phys. Chem.* **1979**, *83*, 2232.

(4) Underwood, A. L.; Anacker, E. W. *J. Phys. Chem.* **1984**, *88*, 2390. (b) *J. Colloid Interface Sci.* **1985**, *106*, 1985.

(5) Imae, T.; Kohsaka, T. *J. Phys. Chem.* **1992**, *96*, 10030.

(6) Shikata, T.; Hirata, H.; Kotaka, T. *Langmuir* **1988**, *4*, 354.

(7) Lin, M. Y.; Hanley, H. J. M.; Sinha, S. K.; Straty, G. C.; Peiffer, D. G.; Kim, M. W. *Phys. Rev. E.* **1996**, *53*, R4302.

(8) Carver, M.; Smith, T. L.; Gee, J. C.; Delichere, A.; Caponetti, E.; Magid, L. J. *Langmuir* **1996**, *12*, 691.

(9) Soltero, J. F. A.; Puig, J. E. *Langmuir* **1996**, *12*, 2654.

(10) Kaler, E. W.; Herrington, K. L.; Murthy, A. K.; Zasadzinski, J. A. N. *J. Phys. Chem.* **1992**, *96*, 6698.

(11) Brown, W.; Johansson, K.; Almgren, M. *J. Phys. Chem.* **1989**, *93*, 5888.

(12) Hassan, P. A.; Valaulikar, B. S.; Manohar, C.; Kern, F.; Bourdieu, L.; Candau, S. *Langmuir* **1996**, *12*, 4350.

(13) Salkar, R. A.; Hassan, P. A.; Samant, S. D.; Valaulikar, B. S.; Kumar, V. V.; Kern, F.; Candau, S. J.; Manohar, C. *J. Chem. Soc., Chem. Commun.* **1996**, 1223.

(14) Kern, F.; Lequeux, F.; Zana, R.; Candau, S. J. *Langmuir* **1994**, *10*, 1714.

(15) Clausen, T. W.; Vinson, P. K.; Minter, J. R.; Davis, H. T.; Talmon, Y.; Miller, W. G. *J. Phys. Chem.* **1992**, *96*, 474.

(16) Candau, S. J.; Khatory, A.; Lequeux, F.; Kern, F. *J. Phys. IV (France)* **1993**, *3*, 197.

(17) (a) Khatory, A.; Lequeux, F.; Kern, F.; Candau, S. J.; *Langmuir* **1993**, *9*, 1456. (b) Appell, J.; Porte, G.; Khatory, A.; Kern, F.; Candau, S. J. *J. Phys. II (France)* **1992**, *2*, 1045. (c) Khatory, A.; Kern, F.; Lequeux, F.; Appell, J.; Porte, G.; Morie, N.; Ott, A.; Urbach, W. *Langmuir* **1993**, *9*, 933.

(18) For an elegant application to CTASal micelles in 0.5 M NaCl, see: Berret, J.-F.; Appell, J.; Porte, G. *Langmuir* **1993**, *9*, 2851. Information on in the entangled regime is not available using scattering methods.

(19) Butler, P. D.; Magid, L. J.; Hamilton, W. A.; Hayter, J. B.; Hammouda, B.; Kreke, P. J. *J. Phys. Chem.* **1996**, *100*, 442.

(20) Hayter, J. B.; Penfold, J. *Colloid Polym. Sci.* **1983**, *261*, 1022.

(21) Imae, T.; Ikeda, S. *Colloid Polym. Sci.* **1987**, *265*, 1090.

(22) Quirion, F.; Magid, L. J. *J. Phys. Chem.* **1986**, *90*, 5435.

(23) Imae, T.; Kamiya, R.; Ikeda, S. *J. Colloid Interface Sci.* **1985**, *108*, 215.

(24) Delsanti, M.; Moussaid, A.; Munch, J. P. *J. Colloid Interface Sci.* **1993**, *157*, 285.

(25) For a theoretical treatment of micellar growth in poorly screened solutions, see: (a) Safran, S.; Pincus, P.; Cates, M. E.; Mackintosh, F. *J. Phys. (Paris)* **1990**, *51*, 503. (b) Mackintosh, F.; Safran, S.; Pincus, P. *Europhys. Lett.* **1990**, *12*, 697.

(26) (a) Porte, G.; Appell, J.; Poggi, Y. *J. Phys. Chem.* **1980**, *84*, 3105. (b) Porte, G.; Appell, J. In *Surfactants in Solution*; Mittal, K. L., Lindman, B., Eds.; Plenum Press: New York, 1983; Vol. 2, p 805.

(27) Swanson-Vethamuthu, M.; Almgren, M.; Karlsson, G.; Bahadur, P. *Langmuir* **1996**, *12*, 2173. Other techniques, such as measurements of ^{1}H NMR line widths (see: Mancini, G.; Schiavo, C.; Cerichelli, G. *Langmuir* **1996**, *12*, 3567) place the sphere-to-rod transition at 1.0−1.5 M NaCl for 0.03 M CTAB.

(28) Hayter, J. B. *Langmuir* **1992**, *8*, 2873.

(29) Morgan, J. D.; Napper, D. H.; Warr, G. G.; Nicol, S. K. *Langmuir* **1994**, *10*, 797.

(30) (a) Manohar, C.; Rao, U. R. K.; Valaulikar, B. S.; Iyer, R. M. *J. Chem. Soc., Chem. Commun.* **1986**, 379. (b) Rao, U. R. K.; Manohar, C.; Valaulikar, B. S.; Iyer, R. M. *J. Phys. Chem.* **1987**, *91*, 3286.

(31) Smith, B. C.; Chou, L. C.; Zakin, J. L. *J. Rheol.* **1994**, *38*, 73.

(32) (a) Bachofer, S. J.; Turbitt, R. M. *J. Colloid Interface Sci.* **1990**, *135*, 325. (b) Bachofer, S. J.; Simonis, U. *Langmuir* **1996**, *12*, 1744.

(33) Kreke, P. J.; Magid, L. J.; Gee, J. C. *Langmuir* **1996**, *12*, 699.

(34) Duffy, D. C.; Davies, P. B.; Bain, C. D. *J. Phys. Chem.* **1995**, *99*, 15241.

(35) Cassidy, M. A.; Warr, G. G. *J. Phys. Chem.* **1996**, *100*, 3237.

(36) Israelachvili, J. N.; Mitchell, D. J.; Ninham, B. W. *J. Chem. Soc., Faraday Trans. 2* **1976**, *72*, 1525.

(37) (a) Hayter, J. B.; Penfold, J. *Mol. Phys.* **1981**, *42*, 109. (b) Hansen, J. P.; Hayter, J. B. *Mol. Phys.* **1982**, *46*, 651.

(38) (a) Nicoli, D. F.; Athanassakis, V.; Moffatt, J. R.; Dorshow, R. B.; Bunton, C. A.; Savelli, G. In *Surfactants in Solution*; Mittal, K. L., Bothorel, P., Eds.; Plenum Press: New York, 1986; Vol. 4, p 203. (b) Ortega, F.; Bacaloglu, R.; McKenzie, D. C.; Bunton, C. A.; Nicoli, D. F. *J. Phys. Chem.* **1990**, *94*, 501.

(39) Baba-Ahmed, L.; Benmouna, M.; Grimson, M. J. *Phys. Chem. Liq.* **1987**, *16*, 235.

(40) Carver, M. Ph.D. Dissertation, University of Tennessee, Knoxville, 1984. The value of 0.36 given in ref 8 is in error.

(41) Gunnarsson, G.; Jönsson, B.; Wennerström, H. *J. Phys. Chem.* **1980**, *84*, 3114.

(42) Drummond, C. J.; Grieser, F.; Healy, T. W. *Faraday Discuss. Chem. Soc.* **1986**, *81*, 95.

(43) Johnson, S. B.; Drummond, C. J.; Scales, P. J.; Nishimura, S. *Langmuir* **1995**, *11*, 2367.

(44) A manuscript on scattering data for these systems at high c_{salt} is in preparation.

(45) This is consistent with the measurement of force vs. separation curves for interacting di-$C_{16}N(CH_3)_2$ bilayers on mica immersed in aqueous Na35ClBz and Na26ClBz. The $35ClBz^-$ ion was found comparable to Sal^- and much more effective than $26ClBz^-$ in its ability to lower ψ_0's. Magid, L. J. In *Ordering and Organizing in Ionic Solutions*; Ise, N., Sogami, I., Eds., World Scientific Publishing Co.: Singapore, 1988; pp 288−301.

(46) The observed shielding for 0.01 M CTA35ClBz is 0.36 ppm, ref 33; assuming $\alpha = 0.1$ gives 0.40 ppm.